Current Biology 23, 2375–2382, December 2, 2013 ©2013 Elsevier Ltd All rights reserved http://dx.doi.org/10.1016/j.cub.2013.10.037

Article

Color Discrimination with Broadband Photoreceptors

Christopher Schnaitmann,[1,5,*] Christian Garbers,[2] Thomas Wachtler,[2,3] and Hiromu Tanimoto[1,4,*]
[1]Max-Planck-Institut für Neurobiologie, 82152 Martinsried, Germany
[2]Department Biology II, Ludwig-Maximilians-Universität München, 82152 Martinsried, Germany
[3]Bernstein Center for Computational Neuroscience Munich, 82152 Martinsried, Germany
[4]Tohoku University Graduate School of Life Sciences, 980-8577 Sendai, Japan

Summary

Background: Color vision is commonly assumed to rely on photoreceptors tuned to narrow spectral ranges. In the ommatidium of *Drosophila*, the four types of so-called inner photoreceptors express different narrow-band opsins. In contrast, the outer photoreceptors have a broadband spectral sensitivity and were thought to exclusively mediate achromatic vision.
Results: Using computational models and behavioral experiments, we demonstrate that the broadband outer photoreceptors contribute to color vision in *Drosophila*. The model of opponent processing that includes the opsin of the outer photoreceptors scored the best fit to wavelength discrimination data. To experimentally uncover the contribution of individual photoreceptor types, we restored phototransduction of targeted photoreceptor combinations in a blind mutant. Dichromatic flies with only broadband photoreceptors and one additional receptor type can discriminate different colors, indicating the existence of a specific output comparison of the outer and inner photoreceptors. Furthermore, blocking interneurons postsynaptic to the outer photoreceptors specifically impaired color but not intensity discrimination.
Conclusions: Our findings show that receptors with a complex and broad spectral sensitivity can contribute to color vision and reveal that chromatic and achromatic circuits in the fly share common photoreceptors.

Introduction

Color vision enables animals to visually discriminate objects based on their spectral properties [1]. It facilitates efficient object recognition, such as identification of food sources or choosing mates [2]. This ability relies on a neuronal comparison of signals from photoreceptors that differ in spectral sensitivity [3]. The compound eye of the fruit fly *Drosophila melanogaster* contains five spectrally different types of photoreceptors, each expressing a single opsin [4]. Each ommatidium contains a set of eight photoreceptors (R1–R8; Figure 1A). The outer photoreceptors (R1–R6) of all ommatidia express the same opsin gene, *rh1* (also known as *ninaE*), and exhibit a two-peaked broadband spectral sensitivity [5, 6] (Figure 1B). These receptors have been considered analogous to vertebrate rod cells [7, 8] and are important for a wide range of achromatic visual behavior, including dim-light vision and motion detection [6–9]. The inner photoreceptors (R7 and R8; Figure 1A) express one of four opsins with different spectral sensitivities [4] (Figure 1B). Opsins Rh3 or Rh4 are expressed in R7, opsins Rh5 or Rh6 in R8, of so-called pale or yellow ommatidia, respectively [4] (Figure 1A). The inner photoreceptors have been shown to function in various visual behaviors, such as phototaxis [10]. Given the single-peaked narrow-band spectral sensitivities of inner photoreceptors, it is commonly assumed that these provide the only input to color vision in flies [7, 11]. However, the respective contributions of the five photoreceptor types to color vision have not been conclusively established [11, 12]. Here we asked whether signals from the broadband photoreceptors and their postsynaptic neurons are used in *Drosophila* to obtain information on the wavelength composition of a visual stimulus.

Results

Behavioral Assay for Color Discrimination in *Drosophila*

While innate phototactic choice has been employed to study spectral preference in *Drosophila* [10, 13, 14], it is unknown whether this behavior is related to color vision [15]. We therefore chose visual discrimination learning—a behavioral paradigm that allows us to control intensity invariance [1, 16–18]. We improved a previously reported conditioning assay in which flies learn to discriminate two colored visual stimuli using sugar reward [19] (Figure S1 available online). Conditioned stimuli were generated by high-power light-emitting diodes (LEDs) with peak intensities at 452 nm (blue) and 520 nm (green), respectively (Figure 1C). While flies significantly discriminate high-intensity blue (bright blue) and green (bright green), it is not clear whether discrimination is based on color or intensity (Figure 1D). Conditioning with differential intensities of either blue or green (1:10 ratio) resulted in significant intensity discrimination (Figure 1D), raising a possibility that the blue/green discrimination might be achromatic.

To ensure that discrimination was based on color, we introduced an intensity mismatch between training and test [18]. Flies were trained with low-intensity blue (dark blue; 10% of bright blue) and bright green, but were tested to discriminate bright blue and bright green. Flies consistently exhibited conditioned approach toward the trained color, despite the 10-fold intensity mismatch (Figure 1E). Similarly, discrimination was not impaired when flies were trained with bright blue/dark green and tested with bright blue/bright green (Figure 1E). Finally, to assess response priority on color and intensity cues [16, 17], we trained flies with dark blue/bright green and tested them with bright blue/dark green, and vice versa (intensity inversion). This experimental design allows us to assess whether flies use a conflicting color or intensity cue [16, 17], as conditioned approach to the color or intensity cue will result in a positive or negative learning index, respectively. Both combinations of the intensity inversion revealed choice priority on the color cue, demonstrating that

[5]Present address: Neurobiologie/Tierphysiologie, Institut für Biologie 1, Albert-Ludwigs-Universität Freiburg, 79104 Freiburg, Germany
*Correspondence: christopher.schnaitmann@biologie.uni-freiburg.de (C.S.), hiromut@m.tohoku.ac.jp (H.T.)

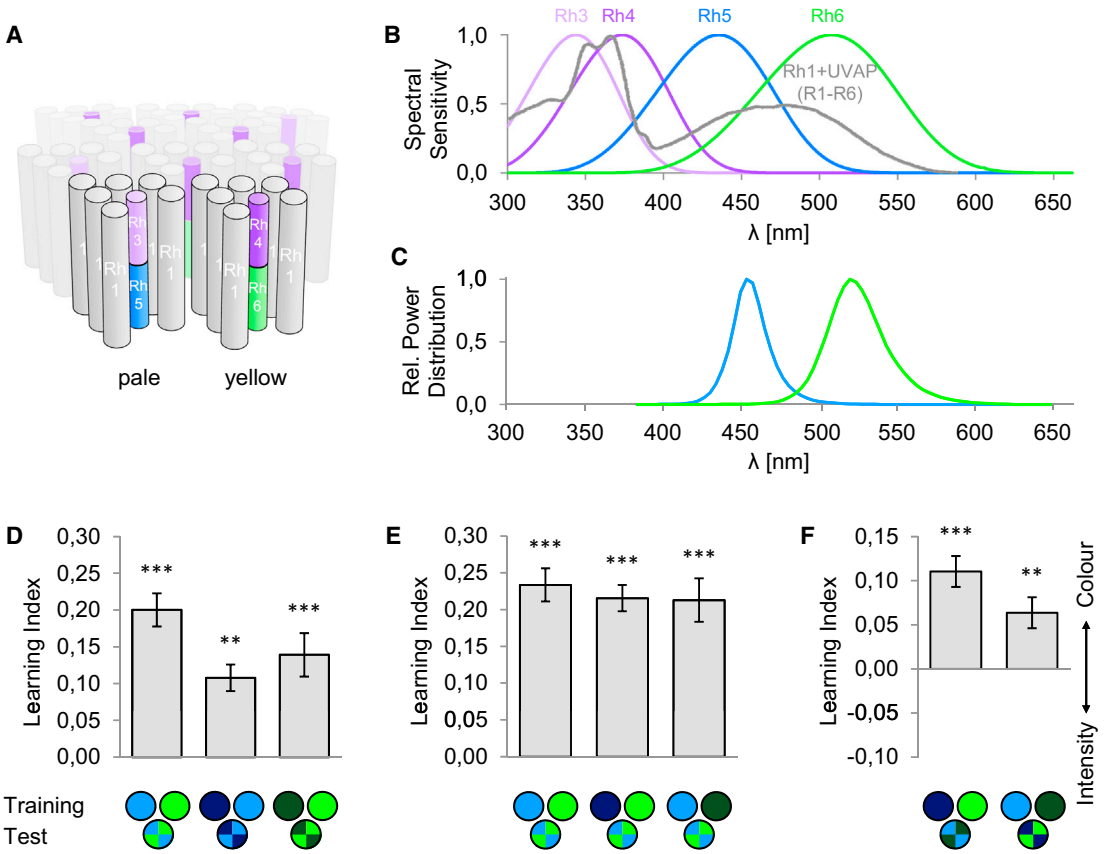

Figure 1. Color Discrimination Learning in *Drosophila*

(A) Composition of opsin types in pale and yellow ommatidia. Six outer photoreceptors (R1–R6; gray) express Rh1. R7 expresses Rh3 or Rh4, and R8 expresses Rh5 or Rh6, depending on the ommatidia class (pale or yellow).

(B) Normalized spectral sensitivities of the different Rhodopsins in the *Drosophila* eye. Rh1 alone is maximally sensitive at 478 nm; an accessory pigment (UVAP) underlies the UV sensitivity of R1–R6 (gray). Data were adapted from [5].

(C) Emission spectra of LEDs used in behavioral experiments.

(D–F) Visual discrimination learning of the fly. Conditioned stimuli, one of which is paired with a sugar reward, and test stimuli are depicted with three circles.

(D) Wild-type flies show significant memory in the bright blue/bright green and in the intensity discrimination tasks (n = 9–18).

(E) Flies choose the color cues despite 10-fold intensity mismatch between training and test (n = 16–20).

(F) Flies show significant color learning despite the conflicting 10-fold intensity inversion between training and test (n = 15–16). Note that intensity learning would result in a negative learning index.

Bars and error bars represent means and SEM, respectively. **p < 0.01; ***p < 0.001; ns, no significance. See also Figure S1.

discrimination was based on spectral composition of conditioned stimuli (Figure 1F).

Broadband Photoreceptors Contribute to Color Discrimination

To determine which photoreceptors feed into color vision, we fitted a model of color opponent processing to experimental results of wavelength discriminability in *Drosophila* [20]. The model predicts discrimination thresholds based on signals in color opponent channels [21]. Variants of the model that included signals from inner receptors gave poor fits to the behavioral data (Figures 2A and 2B), whereas goodness of fit was improved when including the outer photoreceptors (Figure 2C). The superior performance of models including the outer photoreceptors was mainly due to the increasing sensitivity slope of Rh1 in the region around 500 nm, where wavelength discrimination is best (Figure S2). Thus, a contribution of the outer photoreceptors to color vision is necessary to explain the published data on wavelength discrimination in *Drosophila*.

Color Discrimination with Restricted Photoreceptor Sets

To experimentally identify the receptor types responsible for color discrimination, we generated flies with restricted sets of functional photoreceptors. We used blind mutants (*norpA*^{7}) that lack Phospholipase C and restored phototransduction by expressing *norpA*$^{+}$ with different combinations of *rhodopsin-GAL4* drivers [22, 23]. Specificity of GAL4 expression was verified using confocal microscopy (Figures S3A–S3J). To determine functional rescue of photoreceptors, we measured electroretinogram (ERG) responses of the rescue flies with single *rh-GAL4* lines. We used the same LED stimulation as in the conditioning experiments (or UV LED for *rh3-GAL4*) and found that all *norpA* rescues restored light sensitivity (Figures 3A, S3K, and S3L).

We rescued *norpA* in all types of photoreceptors by combining four *rh-GAL4* drivers in the same fly (i.e., *norpA*^{7} *rh1-GAL4/Y; rh5-GAL4 rh6-GAL4/UAS-norpA; rh3+rh4-GAL4/+*) and examined their color-discrimination behavior. The rescue flies fully discriminated bright blue/bright green at the wild-type level (Figure 3B) and exhibited a positive

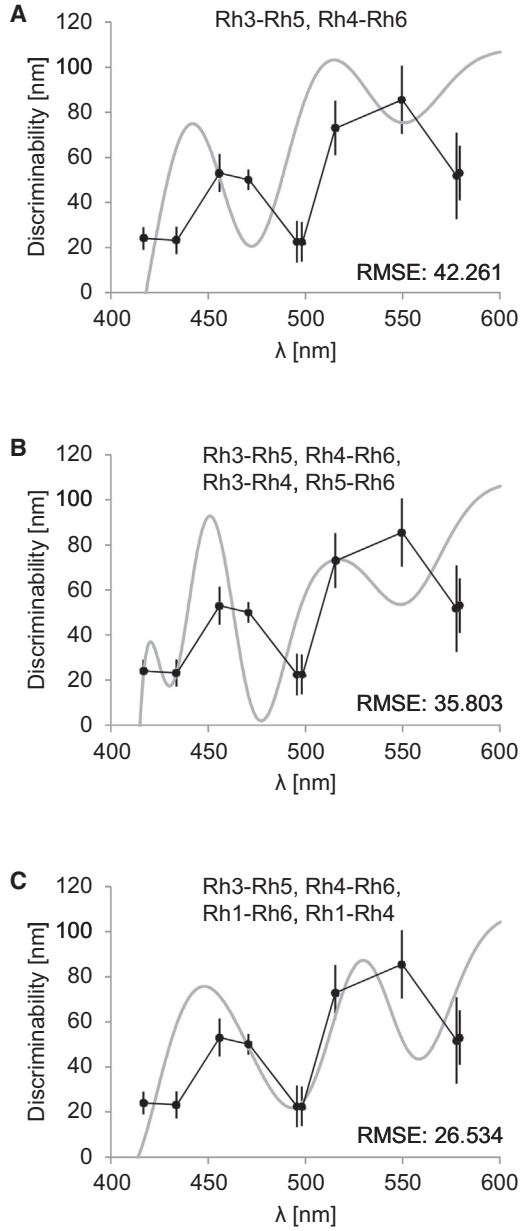

Figure 2. Models of Color Opponent Processing Predict a Contribution of the Outer Photoreceptors to Color Discrimination

Fits of models employing different combinations of color opponent signals (gray curves) to wavelength discrimination in *Drosophila* [20, 21]. Goodness of fit is measured by root-mean-square error corrected for the number of degrees of freedom (RMSE).

(A) Standard model with opponent combinations of inner photoreceptor signals.

(B) The model with the inner photoreceptors including "interommatidial" opponency (i.e., Rh3-Rh4 and Rh5-Rh6) fits slightly better than the standard model.

(C) A model including outer receptor signals achieves a substantially better fit. Note that this model has the same number of parameters as the model in (B). Data points and error bars represent means and SEM, respectively. See also Figure S2.

learning index under intensity inversion, thus demonstrating true color discrimination (Figure 3C). We next generated *norpA* rescue flies in which either all photoreceptors in pale (*rh1-GAL4*, *rh3-GAL4*, and *rh5-GAL4*) or yellow (*rh1-GAL4*, *rh4-GAL4*, and *rh6-GAL4*) ommatidia were functional. Interestingly, the yellow, but not pale, rescue was fully sufficient for bright-blue/bright-green discrimination (Figure 4A). As the sugar preference of the pale rescue flies was not impaired (data not shown), we conclude that pale ommatidia alone are not sufficient for the blue/green discrimination task (Figure 4A). They might play a role for discrimination of other spectral stimulus pairs.

To determine the minimal set of photoreceptors for blue/green discrimination, we generated flies with *norpA* rescue in the three pairwise photopigment combinations in yellow ommatidia (Rh1-Rh4, Rh4-Rh6, and Rh1-Rh6). The combinations of Rh1-Rh4 and Rh4-Rh6 were sufficient for discrimination of bright blue/bright green (Figure 4B), whereas Rh1-Rh6 rescue flies were not able (Figure 4B). Rh1-Rh6 rescue flies did not show color but intensity discrimination in the intensity inversion experiment (Figure 4C). Strikingly, the intensity inversion experiment revealed that both dichromatic combinations of Rh1-Rh4 and Rh4-Rh6 allowed spectral discrimination of blue and green stimuli (Figure 4C). Importantly, the ERG experiments showed that the blue/green intensity ratio is within 10-fold in the rescue with *rh1-GAL4* and *rh6-GAL4*, assuring the successful intensity inversion with dark blue and bright green, and vice versa, at the neural level (Figure S3K). Due to the high blue/green sensitivity ratio of Rh4, the dark blue might be brighter than the bright green for the Rh1-Rh4 rescue flies (Figure S3K), potentially confounding the interpretation of the result (Figure 4C). We therefore performed an intensity inversion experiment where the intensities of dark blue and bright green during training were matched for Rh4 according to the ERG measurements (Figure S3L). Rh1-Rh4 rescue flies still used the color cue under this condition (Figure S4A). Rescue with the single *rh4-GAL4* or without driver did not restore significant color discrimination (Figure S4B), confirming that a neuronal comparison of multiple receptor outputs is required for color vision. Altogether, these results demonstrate that both outer and inner photoreceptors contribute to color vision. The qualitative discrimination difference of the dichromatic rescues in Rh1-Rh4 and Rh1-Rh6 suggests differential computation underlying the signal integration of the outer photoreceptors and the different inner photoreceptor types (i.e., R7 and R8).

The Blockade of Lamina Monopolar Cells Selectively Impairs Color Discrimination

The outer photoreceptors, unlike the other four inner photoreceptors, terminate in the lamina neuropil (Figure 5A). The three lamina monopolar cells (LMCs; L1, L2, and L3) convey the outputs of the outer photoreceptors directly to different layers of the medulla, where visual information of inner and outer photoreceptors converge [24, 25] (Figure 5A). To examine the role of L1–L3 in color discrimination, we blocked the output of these LMCs using ort^{C2}-*GAL4* [14] and *UAS-*shi^{ts1} [26]. Strikingly, this blockade caused a severe impairment in bright-blue/bright-green discrimination (Figure 5B). Intact intensity discrimination showed that appetitive visual memory and behavioral expression were not defective (Figure 5C). As ort^{C2}-*GAL4* additionally labels Dm8, amacrine cells in the medulla that receive R7 output [14] (Figure 5A), we examined a split-GAL4 driver *vglut* ∩ ort^{C2}-*GAL4* to express shi^{ts1} specifically in Dm8 neurons, as well as in a small number of L1 neurons and glia-like cells [14]. These flies did not show any impairment in the bright-blue/bright-green discrimination (Figure 5D). Furthermore, we blocked LMCs with another GAL4

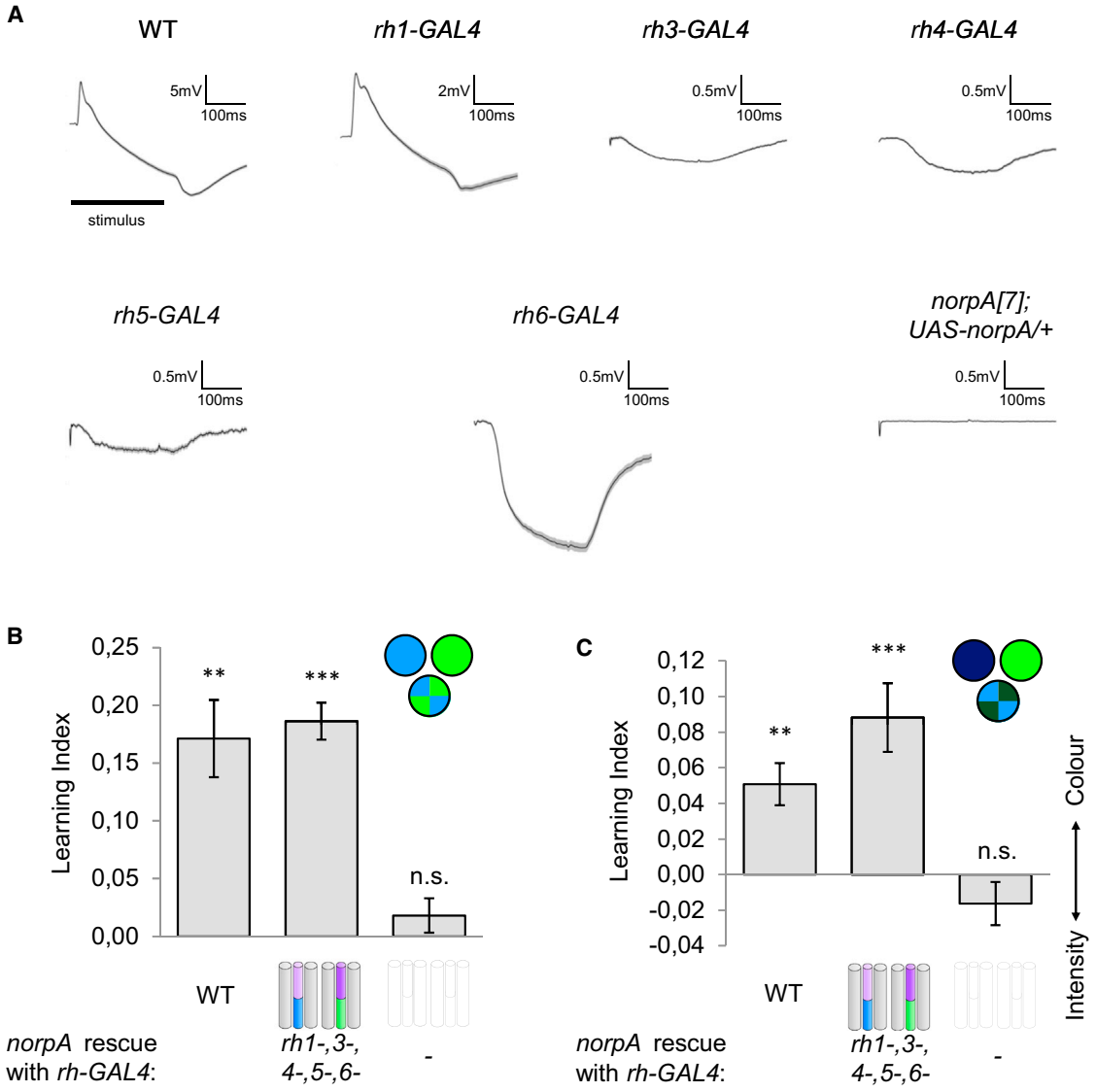

Figure 3. Targeted *norpA* Rescue Restores Photoreceptor Function

(A) ERG traces to dark-blue stimulation of flies with targeted rescues of *norpA* using different *rh-GAL4* drivers (n = 4–8 per genotype). For the rescue with *rh3-GAL4* or without a driver, ERG traces in response to a UV LED (410 nm) or bright blue are plotted, respectively.

(B) The *norpA* rescue in all photoreceptor types fully restores bright-blue/bright-green discrimination learning to the wild-type level, while *norpA* mutant flies containing the rescue construct without driver exhibit no significant discrimination (n = 9–17).

(C) The choice of the rescue flies in all photoreceptors is based on color rather than intensity in the intensity inversion experiment (n = 12–20).

Bars and error bars represent means and SEM, respectively. **p < 0.01; ***p < 0.001; ns, no significance. See also Figure S3.

driver, *R48A08-GAL4*, that strongly labels L1 and L2, as well as two unknown cell types in the medulla [27]. *R48A08-GAL4/UAS-shi^{ts1}* flies were severely impaired in discriminating bright blue and bright green, while their intensity discrimination was intact (Figures 5E and 5F). Thus, we conclude that the LMCs are selectively required for blue/green discrimination.

Discussion

Combining modeling with genetic manipulations and behavioral experiments, we identified the photoreceptor types for blue/green discrimination in *Drosophila* (Figures 4 and S5). Functional color discrimination with the opsin pairs Rh1-Rh4 and Rh4-Rh6 indicates that postreceptoral computations underlying color vision may occur within an optic cartridge deriving from a single ommatidium [28]. Neuronal comparison of differential receptor outputs may be through color opponent mechanisms [29]. TM5 cells in the medulla neuropil are a candidate for color opponent cells comparing Rh1 and Rh4 signals, since they integrate the outputs of LMCs (especially L3) and R7 [14]. Alternatively, the postreceptoral comparisons might take place further downstream in the optic neuropils [30]. Future physiological studies will be necessary to further elucidate this neuronal computation.

Our findings redress the longstanding assumption that solely narrow-band inner photoreceptors mediate color vision [7, 11]. The sensitivity of Rh1 covers a wide spectral range, but it is not uniform (Figure 1B). While this spectral sensitivity is not optimal to represent colors, it nevertheless provides information about differences in wavelength composition. This is in

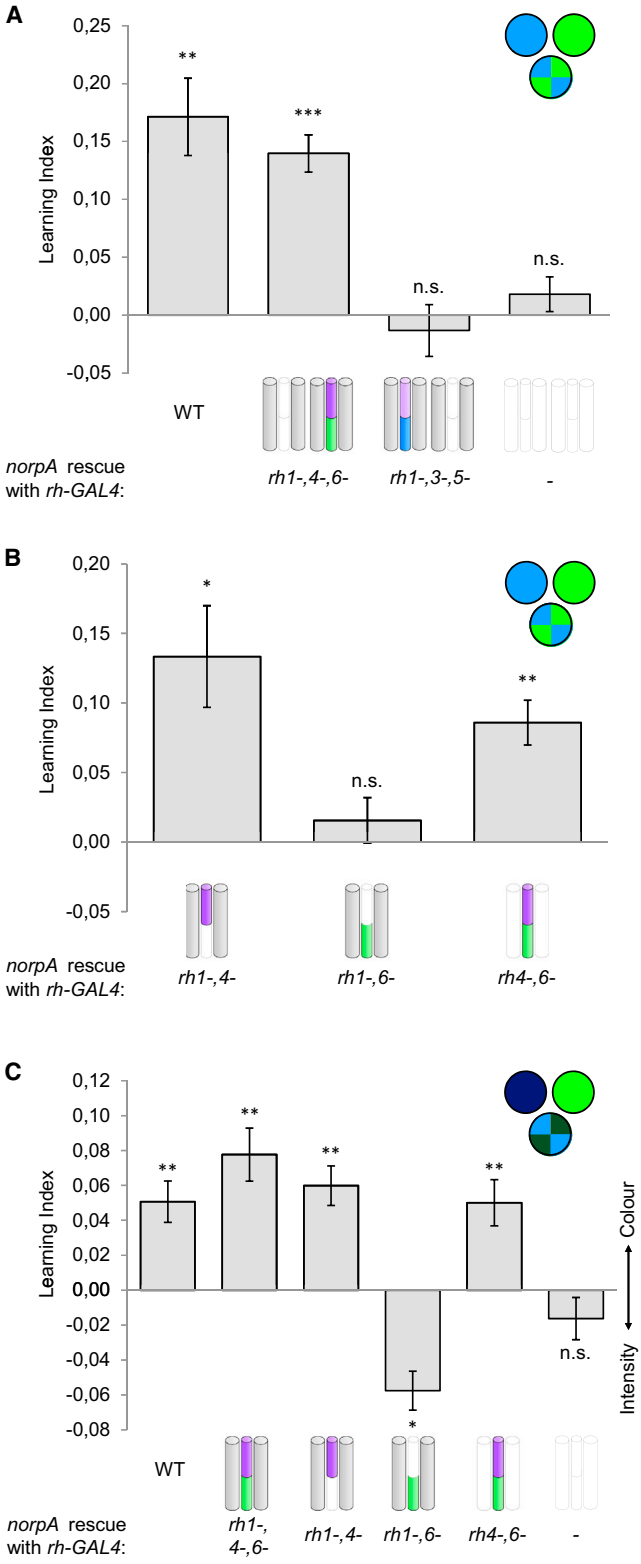

Figure 4. Minimal Sets of Photoreceptors for Color Discrimination

(A) *norpA* rescue flies with functional yellow, but not pale, ommatidia significantly discriminate bright blue and bright green (n = 10–17).

(B) Bright-blue/bright-green discrimination of flies with pairwise *norpA* rescue in yellow ommatidia. Rescue flies with *rh1-GAL4/rh4-GAL4* or *rh4-GAL4/rh6-GAL4* show significant discrimination, while rescue flies with *rh1-GAL4/rh6-GAL4* cannot discriminate the stimuli (n = 8–17).

(C) *norpA* mutants with directed photoreceptor rescues in the intensity inversion task. Pairwise rescues with *rh1-GAL4/rh4-GAL4* or *rh4-GAL4/rh6-GAL4* show significant color preference rather than intensity preference as the wild-type or "yellow rescue" flies. Rescue flies with *rh1-GAL4/rh6-GAL4* significantly choose the intensity cue (n = 12–30).

For wild-type and *norpA[7];UAS-norpA/+* in (A) and (C), the same data are plotted as in Figure 3. Bars and error bars represent means and SEM, respectively. *p < 0.05; **p < 0.01; ***p < 0.001; ns, no significance. See also Figures S4 and S5.

line with the rescued color discrimination with the dichromatic opsin pair Rh1-Rh4 (Figure 4C). Considering the sufficiency of inner photoreceptors for blue/green discrimination (Figures 4 and S5), the role of the outer photoreceptors may be to create an additional opponency dimension for enhanced color discrimination in specific wavelength regions.

The outer photoreceptors have predominant functions in achromatic vision, such as motion detection. Exploitation of the outer photoreceptor pathway for multiple visual functions is advantageous for animals with limited neuronal resources. A recently discovered contribution of *Drosophila* R7/R8 to motion detection corroborates our findings of a differential use strategy [31]. Downstream mechanisms for decoding converged color and motion information await future studies.

Experimental Procedures

Fly Strains

All flies were raised in standard cornmeal medium at 25°C and 60% relative humidity under a 14/10 hr light/dark cycle. The X chromosomes of all transgenic strains were replaced with that of wild-type Canton-S (w^+). Flies were tested 2–6 days after eclosion. For *norpA* rescue experiments, correct genotypes (Table S1) of given crosses were selected before experiments. All rhodopsin GAL4 drivers were kindly provided by Claude Desplan [32]. For *norpA* restoration, *UAS-norpA.K(1)* was used (derived from Bloomington stock number 26267). To test requirement of Rh1, we used a null mutant of *ninaE* (*ninaE*^{8}) with little photoreceptor degeneration [33]. To block the function of neuronal subsets in the lamina neuropil, we crossed the *UAS-shi*^{ts1} [26] line to different driver lines: *+; +; ort*^{C2}*-GAL4* [14] (L1–L3, DM8), *+;vGlut-dVP16AD/CyO; ort*^{C2}*-GAL4DBD/TM6B* [14] (few L1, most DM8), and *R48A08-GAL4* [27] (L1, L2, unknown medulla tangential cell type, unknown proximal medulla cell type; see http://flweb.janelia.org/ for expression pattern [34]). For anatomical analysis, the above driver lines were crossed to *y w; UAS-mCD8::GFP/CyO.*

Behavioral Assay

Flies were trained and tested using a visual appetitive differential conditioning assay [19] with modifications (Figure S1). For narrow-spectral illumination, we constructed a stimulation module using computer-controlled high-power LEDs with peak wavelengths 452 nm and 520 nm (Seoul Z-Power RGB LED) or 456 nm and 520 nm (H-HP803NB, and H-HP803PG, 3W Hexagon Power LEDs, Roithner Lasertechnik) for blue and green stimulation, respectively. LEDs were housed in a base 144 mm below the arena, which allowed homogeneous illumination of a filter paper as a screen. For separate illumination of each quadrant, the light paths of LEDs were separated by light-tight walls in a cylinder with air ducts. "Bright" and "dark" blue and green stimuli were used as explained throughout the manuscript. The intensities were controlled by current and calibrated using a luminance meter BM-9 (Topcon Technohouse) or a PR-655 SpectraScan Spectroradiometer as follows: 0.483 W sr^{-1} m^{-2} (bright blue), 0.048 W sr^{-1} m^{-2} (dark blue), 0.216 W sr^{-1} m^{-2} (bright green), 0.022 W sr^{-1} m^{-2} (dark green), 0.437 W sr^{-1} m^{-2} (Rh4-adapted bright blue), 0.044 W sr^{-1} m^{-2} (Rh4-adapted dark blue), 0.874 W sr^{-1} m^{-2} (Rh4-adapted bright green), and 0.087 W sr^{-1} m^{-2} (Rh4-adapted dark green).

Before experiments, flies were starved at 25°C to a mortality rate of 20%–30% [19]. Flies received four-cycle differential conditioning. Stimulation of the whole arena with one color/intensity was paired with a sucrose reward (2 M) for 1 min, and after a 12 s break in the dark the other color/intensity was presented without reward. The cylindrical arena consisted of a Petri dish (∅ 92 mm; Sarstedt) on which flies could freely move, a pipe wall, and a second Petri dish used for a lid (Figure S1). The pipe's smooth inner

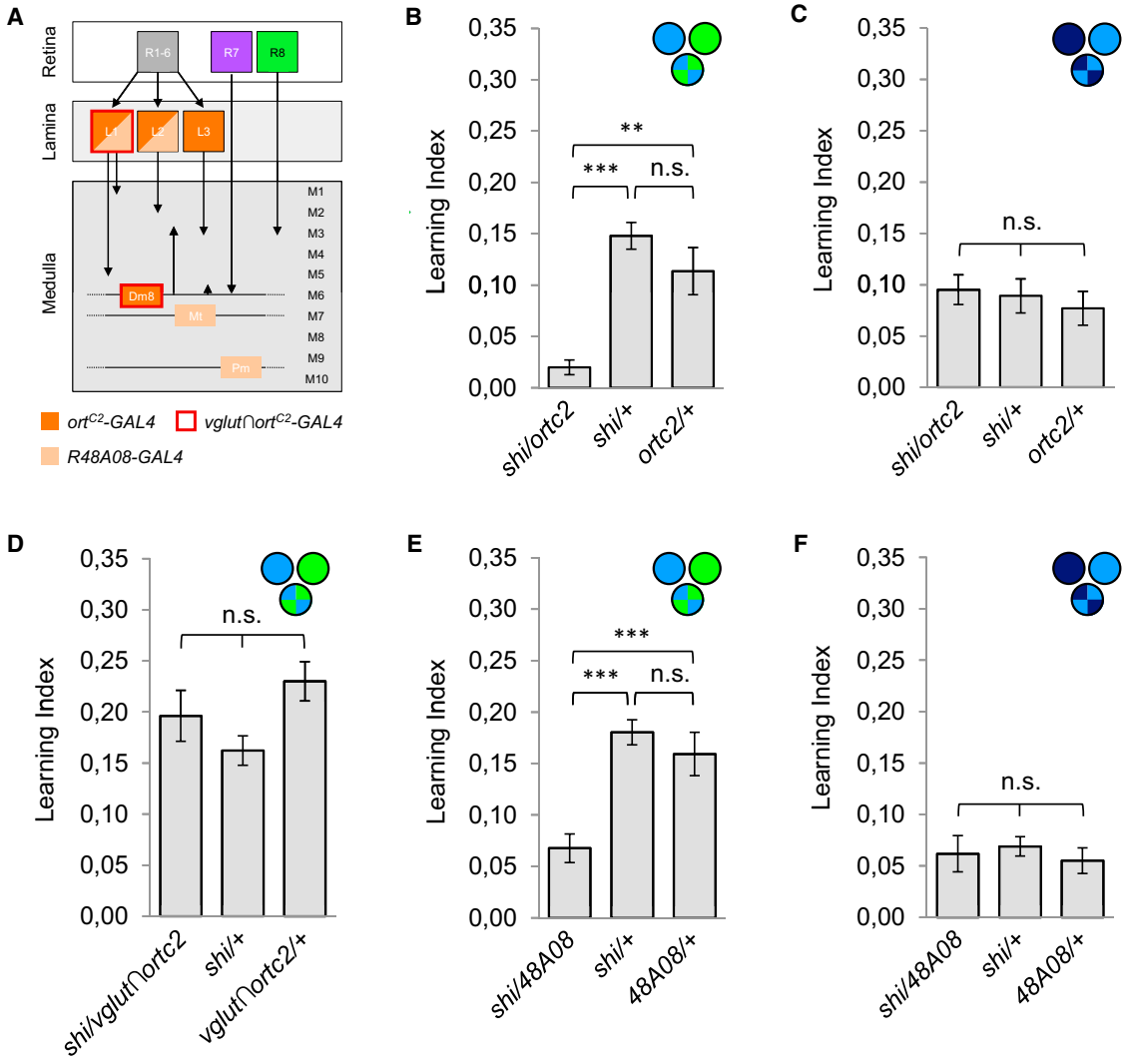

Figure 5. Lamina Monopolar Cells Are Required for Color Discrimination

(A) L1, L2, and L3 receive direct input from the outer photoreceptors R1–R6 and convey their signals to different layers in the medulla. Outputs of inner and outer receptors can converge in the medulla as well as in the downstream lobula complex. Cells labeled by the GAL4 drivers used in the blocking experiments are colored with dark orange or light orange or red outline (Dm8, distal medulla cell type; Mt, medulla tangential cell type; Pm, proximal medulla cell type).

(B) Blocking L1–L3 and Dm8 with Shi^{ts1} and *ort^{C2}-GAL4* specifically impaired bright-blue/bright-green discrimination (n = 13–18).

(C) Intensity discrimination is not impaired with the same blockade (n = 15–16).

(D) Blocking DM8 and a few L1 cells with splitGAL4 driver *vglut ∩ ort^{C2}-GAL4* does not significantly impair bright-blue/bright-green discrimination (n = 12–19).

(E) Bright-blue/bright-green discrimination is significantly impaired by blocking L1, L2, and two other cell types with *R48A08-GAL4* (n = 8–13).

(F) Intensity discrimination is not impaired with the same blockade (n = 17–23).

Bars and error bars represent means and SEM, respectively. **p < 0.01; ***p < 0.001; ns, no significance.

surface and the lid were coated with Fluon (Fluon GP1, Whitford Plastics) to ensure that flies stayed on the filter paper at the bottom of the arena. Reward presentation was switched by inverting the whole arena, tapping the flies gently to detach them from the Petri dish, and exchanging the dishes with sugar or water. In half of the experiments, the reward/no reward sequence was reversed to cancel any effect of order. In the test period, flies were given the choice between two stimuli, presented in two quadrants each.

Conditioned response of the trained flies was recorded with CMOS cameras (FireflyMV, Point Grey Research) for 90 s. The learning index was based on two groups (50–100 flies each), which had been trained reciprocally in terms of the two visual stimuli used. Stimulus preference was determined by the distribution of flies in the arena. A preset macro for ImageJ (W.S. Rasband, US National Institutes of Health) was used to count the number of flies in each quadrant in every frame of our video recordings (90 frames recorded at 1 Hz) [19]. Flies touching a border between two quadrants were excluded.

We calculated a preference index for green (PI_G) for each time point by the difference between the number of flies on the green quadrants and the number on the blue quadrants, divided by the total number of flies counted. PI_G was calculated in both reciprocal experiments (i.e., green rewarded [G+ B−] and blue rewarded [G− B+]):

$$PI_G = \frac{\#Green - \#Blue}{\#Total}$$

A learning index (LI) was calculated by subtraction of PI_G values of the two reciprocally trained groups and by division of the resulting value by 2:

$$LI = \frac{PI_G(G+B-) - PI_G(G-B+)}{2}$$

The LI was calculated for each frame of a recorded video and averaged over the entire test phase (1–90 s), yielding an LI that represented the average performance of the flies. For experiments with *UAS-shi^{ts1}*, flies were trained and tested at 33°C after preincubation at the restrictive temperature for 30 min.

ERG Recordings

ERGs were measured as previously described (C. Garbers et al., 2012, Front. Comput. Neurosci., abstract). In brief, cold-anesthetized flies were attached to a holder with nail polish, which was also used to prevent movement of head and legs. A recording and an indifferent (reference) glass microelectrode filled with 0.1 M KCl were placed just beneath the cornea of the stimulated eye and in the thorax, respectively. The signal recorded at room temperature was amplified using an Intronix 2015f amplifier and digitally acquired using a NI PCI-6025E data acquisition board. Visual stimulation from the behavioral experiments (dark blue or bright green) was reproduced by using the same LEDs, intensities, and filter paper screen. Data acquisition and stimulation were controlled with the Relacs toolbox [35]. Using a modified closed-loop light clamp technique [36], wild-type and *norpA*-rescue flies were analyzed for their spectral sensitivity ratio for blue and green LEDs. As an internal reference of the interleaved ERG (INTER ERG) (C. Garbers et al., 2012, Front. Comput. Neurosci., abstract), we used the response to the blue LEDs set to the "dark" intensity as in the behavioral experiments. Using an iteratively updated linear regression model, the intensity of the green LED was adjusted to the level that evoked the same ERG response as the blue reference LED. The ERG response was defined as the difference in the average signals 10 ms before stimulation onset and 10 ms before offset. The stimulation protocol consisted of a 100 ms green light followed by 500 ms of no stimulation before 100 ms of the blue reference light followed by 500 ms of no stimulation. An average response difference to the blue reference was calculated based on five cycles of the stimulation protocol, and the measurement was repeated until the difference reached less than 4% of the reference amplitude. At least eight measurements in two flies were done per genotype. Blue/green intensity ratios were calculated by normalization of the dark-green stimulus with the green LED intensity producing the same signal amplitude as the reference (dark blue).

Immunohistochemistry and Microscopy

The retina of flies was prepared in agarose sections [37]. In brief, heads were fixed in 4% formaldehyde in PBT (PBS and 0.3% Triton X-100), embedded in 7% agarose (Biomol), and sectioned horizontally at 80 μm with a vibrating microtome (Leica VT 1000S). Agarose sections were bleached in 0.1% $NaBH_4$ for 30 min to reduce autofluorescence of the red eye pigment and were subsequently blocked with 3% normal goat serum for 30 min at room temperature. Preparations were incubated overnight at 4°C with the antibodies against GFP (1:1000) and Rh6 (a gift from Claude Desplan; 1:5,000) in the blocking solution. After washing with PBT, slices were incubated overnight at 4°C with AlexaFluor-568- and AlexaFluor-633-conjugated secondary antibodies in the blocking solution. Preparations were rinsed and mounted in Vectashield (Vector Laboratories). Confocal stacks were collected with Olympus FV-1000 microscope (Olympus). Image processing was performed with ImageJ.

Modeling Wavelength Discrimination

To compare spectral discrimination abilities, we calculated the contrast that two stimuli evoke at a hypothetical postreceptor neuronal stage [21]. For two stimuli, let $\Delta q_i(\lambda)$ be the difference in excitation for receptor i at wavelength λ. Then for two receptor types 1 and 2, the signal contrast in a neuronal channel k that combines these two receptor signals opponently can be written as

$$\Delta S_k^2(\lambda) = (\Delta q_1(\lambda) - \Delta q_2(\lambda))^2. \qquad \text{(Equation 1)}$$

To predict discrimination for a visual system combining information from more than one opponent channel, we sum over the k respective mechanisms:

$$\Delta S^2(\lambda) = \sum_{k=0}^{n} w_k S_k^2(\lambda), \qquad \text{(Equation 2)}$$

where w_k is a vector of weights that scale the channels relative to each other. For the special case of wavelength discrimination, $\Delta q_i(\lambda)$ corresponds to the slope of the receptor spectral sensitivity of receptor i at wavelength λ. Calculation of this relative discrimination at each wavelength λ yields an estimate of the spectral sensitivity function. We fitted this function to the data [21] by adjusting *w* such that the resulting squared differences between the estimates and the data were minimized. Goodness of fit was calculated via the chi-square statistic, treating the data [20] as normally distributed.

Statistics

Statistical analyses were performed with the use of Prism (GraphPad Software). If groups did not violate the assumption of normal distribution, one sample t tests were used to test difference from zero. Otherwise, a nonparametric Wilcoxon signed rank test was employed. p values of both tests were Bonferroni corrected. For comparison of groups, none of which violated the assumption of normal distribution or homogeneity of variance, mean performance indices were compared with a one-way ANOVA followed by planned multiple pairwise comparisons (Bonferroni correction). Where comparisons with multiple control groups gave distinct significance levels, only the most conservative result is shown.

Supplemental Information

Supplemental Information includes five figures and one table and can be found with this article online at http://dx.doi.org/10.1016/j.cub.2013.10.037.

Acknowledgments

We thank A. Eckart, A.B. Friedrich, C. O'Brien, K. Öchsner, S. Prech, I. Siwanowicz, and B. Tepe for excellent technical assistance and C. Desplan for anti-Rh6 antibody and T. Clandinin, C. Desplan, C.-H. Lee, M. Heisenberg, M. Juusola, W. Pak, and the Bloomington Stock Center for fly stocks. We also thank M. Jösch-Krotki for pilot ERG measurements. We thank J. Benda and J. Grewe for technical support regarding ERG measurements. We are grateful to A. Borst, D. Reiff, and H.-C. Spatz for discussion and critical reading of the manuscript. C.S. received a doctoral fellowship from Boehringer Ingelheim Fonds. This work was supported by Bundesministerium für Bildung und Forschung through Bernstein Focus Neurobiology of Learning (01GQ0932) and Bernstein Center for Computational Neuroscience Munich (01GQ1004A) and by Max-Planck-Gesellschaft.

Received: August 24, 2013
Revised: October 14, 2013
Accepted: October 15, 2013
Published: November 21, 2013

References

1. Kelber, A., Vorobyev, M., and Osorio, D. (2003). Animal colour vision—behavioural tests and physiological concepts. Biol. Rev. Camb. Philos. Soc. *78*, 81–118.
2. Osorio, D., and Vorobyev, M. (2008). A review of the evolution of animal colour vision and visual communication signals. Vision Res. *48*, 2042–2051.
3. Rushton, W.A.H. (1972). Pigments and signals in colour vision. J. Physiol. *220*, 1P–31P.
4. Rister, J., Desplan, C., and Vasiliauskas, D. (2013). Establishing and maintaining gene expression patterns: insights from sensory receptor patterning. Development *140*, 493–503.
5. Salcedo, E., Huber, A., Henrich, S., Chadwell, L.V., Chou, W.-H., Paulsen, R., and Britt, S.G. (1999). Blue- and green-absorbing visual pigments of Drosophila: ectopic expression and physiological characterization of the R8 photoreceptor cell-specific Rh5 and Rh6 rhodopsins. J. Neurosci. *19*, 10716–10726.
6. Hardie, R.C. (1985). Functional organization of the fly retina. Prog. Sens. Physiol. *5*, 1–79.
7. Pichaud, F., Briscoe, A., and Desplan, C. (1999). Evolution of color vision. Curr. Opin. Neurobiol. *9*, 622–627.
8. Strausfeld, N.J., and Lee, J.-K. (1991). Neuronal basis for parallel visual processing in the fly. Vis. Neurosci. *7*, 13–33.
9. Yamaguchi, S., Wolf, R., Desplan, C., and Heisenberg, M. (2008). Motion vision is independent of color in Drosophila. Proc. Natl. Acad. Sci. USA *105*, 4910–4915.
10. Yamaguchi, S., Desplan, C., and Heisenberg, M. (2010). Contribution of photoreceptor subtypes to spectral wavelength preference in Drosophila. Proc. Natl. Acad. Sci. USA *107*, 5634–5639.
11. Troje, N. (1993). Spectral categories in the learning behaviour of blowflies. Z. Naturforsch. Teil C Biochem. Biophys. Biol. Virol. *48*, 96.
12. Fukushi, T. (1994). Colour perception of single and mixed monochromatic lights in the blowfly Lucilia cuprina. J. Comp. Physiol. A *175*, 15–22.

13. Fischbach, K.F. (1979). Simultaneous and successive colour contrast expressed in "slow" phototactic behaviour of walking Drosophila melanogaster. J. Comp. Physiol. A *130*, 161–171.
14. Gao, S., Takemura, S.Y., Ting, C.-Y., Huang, S., Lu, Z., Luan, H., Rister, J., Thum, A.S., Yang, M., Hong, S.-T., et al. (2008). The neural substrate of spectral preference in Drosophila. Neuron *60*, 328–342.
15. Menzel, R., and Greggers, U. (1985). Natural phototaxis and its relationship to colour vision in honeybees. J. Comp. Physiol. A *157*, 311–321.
16. Bicker, G., and Reichert, H. (1978). Visual learning in a photoreceptor degeneration mutant of Drosophila melanogaster. J. Comp. Physiol. A *127*, 29–38.
17. Tang, S., and Guo, A. (2001). Choice behavior of Drosophila facing contradictory visual cues. Science *294*, 1543–1547.
18. Menne, D., and Spatz, H.-C. (1977). Colour vision in Drosophila melanogaster. J. Comp. Physiol. A *114*, 301–312.
19. Schnaitmann, C., Vogt, K., Triphan, T., and Tanimoto, H. (2010). Appetitive and aversive visual learning in freely moving Drosophila. Front Behav Neurosci *4*, 10.
20. Hernandez de Salomon, C., and Spatz, H.C. (1983). Colour vision in Drosophila melanogaster: wavelength discrimination. J. Comp. Physiol. A *150*, 31–37.
21. Vorobyev, M., and Osorio, D. (1998). Receptor noise as a determinant of colour thresholds. Proc. Biol. Sci. *265*, 351–358.
22. Inoue, H., Yoshioka, T., and Hotta, Y. (1985). A genetic study of inositol trisphosphate involvement in phototransduction using Drosophila mutants. Biochem. Biophys. Res. Commun. *132*, 513–519.
23. Wernet, M.F., Velez, M.M., Clark, D.A., Baumann-Klausener, F., Brown, J.R., Klovstad, M., Labhart, T., and Clandinin, T.R. (2012). Genetic dissection reveals two separate retinal substrates for polarization vision in Drosophila. Curr. Biol. *22*, 12–20.
24. Fischbach, K., and Dittrich, A. (1989). The optic lobe of Drosophila-melanogaster 0.1. a Golgi analysis of wild-type structure. Cell Tissue Res. *258*, 441–475.
25. Meinertzhagen, I.A., and O'Neil, S.D. (1991). Synaptic organization of columnar elements in the lamina of the wild type in Drosophila melanogaster. J. Comp. Neurol. *305*, 232–263.
26. Kitamoto, T. (2001). Conditional modification of behavior in Drosophila by targeted expression of a temperature-sensitive shibire allele in defined neurons. J. Neurobiol. *47*, 81–92.
27. Tuthill, J.C., Nern, A., Holtz, S.L., Rubin, G.M., and Reiser, M.B. (2013). Contributions of the 12 neuron classes in the fly lamina to motion vision. Neuron *79*, 128–140.
28. Morante, J., and Desplan, C. (2008). The color-vision circuit in the medulla of Drosophila. Curr. Biol. *18*, 553–565.
29. Menzel, R., and Backhaus, W. (1989). Color Vision Honey Bees: Phenomena and Physiological Mechanisms (Berlin: Springer-Verlag).
30. Kien, J., and Menzel, R. (1977). Chromatic properties of interneurons in the optic lobes of the bee. II. Narrow band and colour opponent neurons. J. Comp. Physiol. A *113*, 35–53.
31. Wardill, T.J., List, O., Li, X., Dongre, S., McCulloch, M., Ting, C.-Y., O'Kane, C.J., Tang, S., Lee, C.-H., Hardie, R.C., and Juusola, M. (2012). Multiple spectral inputs improve motion discrimination in the Drosophila visual system. Science *336*, 925–931.
32. Mollereau, B., Wernet, M.F., Beaufils, P., Killian, D., Pichaud, F., Kühnlein, R., and Desplan, C. (2000). A green fluorescent protein enhancer trap screen in Drosophila photoreceptor cells. Mech. Dev. *93*, 151–160.
33. Kumar, J.P., and Ready, D.F. (1995). Rhodopsin plays an essential structural role in Drosophila photoreceptor development. Development *121*, 4359–4370.
34. Jenett, A., Rubin, G.M., Ngo, T.-T.B., Shepherd, D., Murphy, C., Dionne, H., Pfeiffer, B.D., Cavallaro, A., Hall, D., Jeter, J., et al. (2012). A GAL4-driver line resource for Drosophila neurobiology. Cell Rep *2*, 991–1001.
35. Benda, J., Gollisch, T., Machens, C.K., and Herz, A.V. (2007). From response to stimulus: adaptive sampling in sensory physiology. Curr. Opin. Neurobiol. *17*, 430–436.
36. Franceschini, N. (1979). Voltage Clamp by Light - Rapid Measurement of the Spectral and Polarization Sensitivities of Receptor-Cells. Invest. Ophthalmol. Vis. Sci. *18* (*Suppl.*), 5.
37. Gruber, F., Knapek, S., Fujita, M., Matsuo, K., Bräcker, L., Shinzato, N., Siwanowicz, I., Tanimura, T., and Tanimoto, H. (2013). Suppression of conditioned odor approach by feeding is independent of taste and nutritional value in Drosophila. Curr. Biol. *23*, 507–514.